Effective potential and local density approximation approach to the binding energy of closed shell nuclei

M. Modarres* and N. Rasekhinejad
Physics Department, University of Tehran, 1439955961, Tehran, Iran
(Received 2 May 2005; published 7 July 2005)

The ground state binding energies of closed shell nuclei such as ^{4}He, ^{12}C, ^{16}O, ^{28}Si, ^{32}S, ^{40}Ca, and ^{56}Ni are calculated by using the local density approximation in the harmonic oscillator basis. Different channel effective two-body interactions are generated from the lowest order constrained variational calculation for nuclear matter with the Reid68 and Δ-Reid68 potentials. It is shown that the unlike nuclear matter, Reid68 potential gives ground state binding energies closer to the experimental data with respect to the Δ-Reid68 interaction. The different channel effective interactions as well as one- and two-body density distribution functions are discussed and compared with the results of other approaches such as the correlated basis function, variational fermion hypernetted chain, variational cluster Monte Carlo, Brueckner-Hartree-Fock, fermionic molecular dynamics, and coupled cluster.

DOI: 10.1103/PhysRevC.72.014301 PACS number(s): 21.60.Gx, 21.10.Dr, 27.20.+n, 27.40.+z

I. INTRODUCTION

The simplest model for a nucleus is a collection of point nucleons that obey the independent particle models, i.e., shell models. But it is now understood that the nucleus wave function is largely deviated from this traditional approximation because of the complicated, strong, short-range nucleon-nucleon interaction. At present, several N-N potentials are available and most of them fit reasonably well the deuteron and nucleon-nucleon scattering phase shift data. Handling such complicated potentials in the nuclear system, however, has been a great task for many-body theorists during the last five decades.

Recently, the situation has changed for few-body nucleon systems, i.e., $A = 3 - 7$. The Faddeev, Green's function Monte Carlo, and correlated hyperspherical harmonics expansion (CHHE) [1] theories have been developed, and satisfactory results have been reproduced. The $A > 7$ light nuclei (up to ^{16}O) have been described by the variational or cluster Monte Carlo (VMC, CMC) technique by using the Jastrow variational wave function [2]. The VMC or CMC formalism is very involved, and its accuracy is uncertain (ignoring 3, 4, ... cluster terms, the choice of the Jastrow correlation functions especially with no center-of-mass dependence, uncertainty in the values of normalization integral up to 10%, etc., for example, in ^{16}O [2]). So it cannot yet be considered an exact or reliable formalism such as Green's function Monte Carlo technique.

For infinite nucleonic matter, we do not have a finite size problem, but one needs a reliable many-body technique and a true nucleon-nucleon potential to get reliable results.

Several of our works [3] noted that the many-body calculations on nuclear matter with phenomenological interactions such as the Reid68 [3] potential which fit the two-nucleon data give substantially too much binding and saturate the nuclear matter at densities that are too high. This problem was reported by different groups during the last three decades [4,5].

In 1979 [3,6], we included the $NN \rightarrow N\Delta$ transition potential explicitly in the Hamiltonian, by modifying the Reid68 potential (Δ-Reid68) [3], from the beginning and considered the isobar degree of freedom in our trial variational wave function. The result of the lowest order constrained variational (LOCV) calculation [3,6], with the above transition potential and corresponding trial wave function, was shown to give a reasonable binding and saturation density for nuclear matter.

Since then, a few sophisticated interactions such as the UV_{14} [7], AV_{14} [8], and new Argonne AV_{18} [9], as well as Reid93 [10] potentials, have been generated and used. These potentials fit the N-N scattering data very well [10]. But all of them still overbind nuclear matter at large saturation densities. On the other hand, a very good agreement was found between results of the LOCV technique [11,12] and those of more sophisticated methods such as variational fermion hypernetted chain (FHNC) calculations [11,12], at both zero and finite temperatures. The three-body cluster contribution to the nuclear matter energy and the normalization integral $\langle\psi|\psi\rangle$ were calculated to test the convergence of cluster expansion truncation [12]. It was shown that the LOCV technique is capable of dealing with the well-defined phenomenological potentials. However, as we said before, most of these works found that all of the new potentials, like the old Reid68 potential, overbind nuclear matter at larger density than the empirical prediction.

The LOCV method has also been applied to finite nuclei [13], for which there was some difficulty in defining the long-range behavior of the correlation functions. Since the cluster expansion will not converge reasonably because of certain restrictions on the correlation functions, which cannot be satisfied by the inhomogeneous systems, then one should ignore higher cluster terms; this is not a valid assumption

*Corresponding author, e-mail: modarres@khayam.ut.ac.ir

especially for light nuclear systems, etc. The results of LOCV calculation for the light closed shell nuclei were not satisfactory [13].

To overcome this difficulty, in the spirit of the local density $\mathcal{G}$ matrix, in 1984, we generated the effective two-body channel interactions from our LOCV nuclear matter calculation at different densities, and then we converted this dependence to a local one by some fitting approximation [14] to calculate properties of the ^{4}He nucleus. The result was encouraging, but we needed much more computer time (which was not available for us in the 1980s) to extend this model to heavier nuclei and eliminate the fitting approximations.

With respect to the above arguments, in this work we will attempt to calculate the properties of light closed shell nuclei such as ^{4}He, ^{12}C, ^{16}O, ^{28}Si, ^{32}S, ^{40}Ca, and ^{56}Ni in the harmonic oscillator basis by using a local density approximation and the effective two-body channel-dependent potentials which have been generated through the LOCV formalism with the Reid68 and Δ-Reid68 interactions. We also try to eliminate the approximations that we made in our previous work [14]. Then we can compare the present results with those of the coupled cluster method (CCM) [15], correlated basis function (CBF-FHNC) [16], variational or cluster Monte Carlo (VMC, CMC) [2], Brueckner-Hartree-Fock (BHF) [17], and fermionic molecular dynamics (FMD) [18] calculations which have been presented recently, most of which need enormous computational time on super or mainframe computers. A comparison is also made with the present available data [19].

By using our asymmetrical nuclear matter code, we hope in the near future to develop this technique for the heavier nuclei with different numbers of protons and neutrons with more realistic single-particle states such as those of the Woods-Saxon potential.

In this article, we do not intend to use the recent phenomenological potentials such as AV_{18} [9] since in our previous calculations we found that these potentials do not correctly predict the empirical saturation properties of nuclear matter [12], and they are not much different from the old Reid68 potential. This point has been also reported by other groups [11,16,17]. However, we should mention that in 1993, the properties of various N-N interactions were investigated by the Nijmegen group [20], and their final report indicated that the AV_{18} (charge-dependent version of the AV_{14}) [9], the Nijm I and II [20], and the update version of the Reid68 [10,20], Reid93, are truly N-N interactions, i.e., they give an excellent description of both the *pp* and *np* scattering data simultaneously. The Reid68 potential [3] fitted the *pp* data very well, but not the *np* data. We do not know how good the Δ-Reid68 interaction [5] is. According to the Helsinki group [21], they modified the Reid68 $^1S_0$ interaction by including the $^1S_0$-$^5D_0$ transition potential such that they obtain the correct N-N $^1S_0$ scattering phase shift. Furthermore, as we pointed out before, this potential can predict the nuclear matter saturation properties closer to the empirical values than do the other potentials. It also takes into the account the well-known Pauli and mean-field effects of the intermediate N-Δ state [22], which can be the origin of three-body forces. However, our recent work on nuclear matter [23] shows that the new Reid potential, Reid93, overbinds nuclear matter at much higher saturation density than does Reid68 (as explained in [23], there are discrepancies between our results using Reid93 and those from BHF). Nevertheless, both Reid68 and Reid93 potentials give similar saturation properties for nuclear matter up to $J = 2$ channels [23]. On the other hand, as we said before, the present available calculations on finite nuclei show that the nucleus properties, unlike nuclear matter, are not very sensitive to the choice of potential [16,17] (especially for light nuclei). One reason could be the low-density properties of nuclei compared to nuclear matter (the long-range parts of different N-N potentials are roughly the same, and there is always a balance between the central and tensor components of the N-N forces).

So the paper is planned as follows: A short description of the lowest order constrained variational method and the calculation of effective potentials are given in Sec. II. Section III is devoted to the evaluation of matrix elements and energy of different closed shell nuclei obtained by using the local density approximation. Finally, in Sec. IV, we present the results and discussions.

II. THE LOCV FORMALISM AND EFFECTIVE POTENTIALS

In the LOCV method, we use an ideal Fermi gas type of wave function for the single-particle states and variational techniques to find the wave function of the interacting system [3,12], i.e.,

$$\psi = \mathcal{F}\Phi, \tag{1}$$

where

$$\mathcal{F} = \mathcal{S}\prod_{i>j} F(ij), \tag{2}$$

with $\mathcal{S}$ a symmetrizing operator. The correlation functions $F(ij)$ are operators and written as

$$F(ij) = \sum_{\alpha,k} f_\alpha^{(k)}(ij)O_\alpha^{(k)}(ij). \tag{3}$$

In the above equation, $\alpha = \{S, L, J, T\}$, $k = 1, 4$, and

$$O_\alpha^{k=1,4} = 1, \left(\tfrac{2}{3} + \tfrac{1}{6}S_{12}^I\right), \left(\tfrac{1}{3} - \tfrac{1}{6}S_{12}^I\right), S_{12}^{II}. \tag{4}$$

For spin-singlet channels with orbital angular momentum $L \neq 0$ and the spin-triplet channels with $L \neq J \pm 1, k$ is superfluous and set only to unity; while for $L = J \pm 1$, it takes values of 2 and 3. It remains the $L = 0$ channel which couples the $^1S_0$ channel to the $^5D_0$ channel. In this case, we set $k = 1$ and 4.

In general, the N-Δ correlation function $f_\alpha^{(4)}$ is required to heal to zero while the rest of the channel correlation functions $f_\alpha^{(1)}$, $f_\alpha^{(2)}$, and $f_\alpha^{(3)}$ heal to the modified Pauli function $f_P(r)$,

$$f_P(r) = [1 - l(k_F r)^2]^{-\frac{1}{2}}, \tag{5}$$

with

$$l(x) = \frac{3}{2x}\mathcal{J}_1(x), \tag{6}$$

where $\mathcal{J}_J(x)$ are the familiar spherical Bessel functions and the Fermi momenta k_F are fixed by the nuclear matter density, i.e., $k_F = (\frac{3\pi^2}{2}\rho)^{\frac{1}{3}}$.

The nuclear matter energy per nucleon is [3,12],

$$E_{\rm in} = T_F + E_{\rm MB}[F]. \tag{7}$$

T_F is simply the Fermi gas kinetic energy, and it is written as

$$T_F = \frac{3}{5}\frac{\hbar^2 k_F^2}{2m}. \tag{8}$$

The many-body energy term $E_{\rm MB}[F]$ is calculated by constructing a cluster expansion for the expectation value of our Hamiltonian,

$$H = \sum_i \frac{{p_i}^2}{2m} + \sum_{i>j} V_{ij}, \tag{9}$$

where V_{ij} is the bare N-N interaction. Then, we keep only the first two terms in a cluster expansion of the energy functional

$$E[F] = \frac{1}{A}\frac{\langle\Psi|H|\Psi\rangle}{\langle\Psi|\Psi\rangle} = T_F + E_{\rm MB} = T_F + E_2 + E_3 + \cdots. \tag{10}$$

The two-body energy term is defined as

$$E_2 = (2A)^{-1}\sum_{ij}\langle ij|\mathcal{V}(12)|ij\rangle_a, \tag{11}$$

where

$$\mathcal{V}(12) = -\frac{\hbar^2}{2m}\left\{F(12),\left[\nabla_{12}^2, F(12)\right]\right\} + F(12)V(12)F(12), \tag{12}$$

and the two-body antisymmetrized matrix element $\langle ij|\mathcal{V}|ij\rangle_a$ are taken with respect to the single-particle functions composing Φ, i.e., the plane waves. In LOCV formalism, $E_{\rm MB}$ is approximated by E_2, and one hopes that the normalization constraint makes the cluster expansion converge very rapidly and bring the many-body effect into the E_2 term.

By inserting a complete set of two-particle states twice in Eq. (11) and performing some algebra, we can rewrite the two-body term as

$$E_2 = E_c^{NN} + E_{\mathcal{T}}^{NN} + E_{\mathcal{T}}^{N\Delta}, \tag{13}$$

where c and $\mathcal{T}$ stand for the central and tensor parts, respectively, then

$$E_i^j = \frac{2}{\pi^4\rho}\sum_\alpha (2T+1)(2J+1)\frac{1}{2}\{1-(-1)^{L+S+T}\} \times \int_0^\infty r^2 dr\, \mathcal{V}_\alpha^{i,j}(r,\rho)a_\alpha^{(1)^2}(r), \tag{14}$$

and ($i = c, \mathcal{T}$ and $j = NN, N\Delta$)

$$\mathcal{V}_\alpha^{c,NN}(r,\rho) = \frac{\hbar^2}{m}\left\{f_\alpha^{(1)^2} + \frac{m}{\hbar^2}V_\alpha^c f_\alpha^{(1)^2}\right\}, \tag{15}$$

$$\begin{aligned}\mathcal{V}_\alpha^{\mathcal{T},NN}(r,\rho) &= \left\{\frac{\hbar^2}{m}\left[f_\alpha^{(2)^2} + \frac{m}{\hbar^2}\left(V_\alpha^c + 2V_\alpha^{\mathcal{T}} - V_\alpha^{LS}\right)f_\alpha^{(2)^2}\right]a_\alpha(r)^{(2)^2}\right. \\ &+ \frac{\hbar^2}{m}\left[f_\alpha^{(3)^2} + \frac{m}{\hbar^2}\left(V_\alpha^c - 4V_\alpha^{\mathcal{T}} - 2V_\alpha^{LS}\right)f_\alpha^{(3)^2}\right]a_\alpha^{(3)^2}(r) \\ &\left.+\left[r^{-2}\left(f_\alpha^{(2)^2} - f_\alpha^{(3)^2} + \frac{m}{\hbar^2}V_\alpha^{LS}f_\alpha^{(2)}f_\alpha^{(3)}\right)\right]b_\alpha^2\right\}a_\alpha^{(1)^{-2}}(r)\end{aligned} \tag{16}$$

$$\begin{aligned}\mathcal{V}_\alpha^{\mathcal{T},N\Delta}(r,\rho) = \left\{\frac{\hbar^2}{2\mu}\left[f_\alpha^{(1)^2} + \frac{\mu}{\mu_\Delta}\left(f_\alpha^{(4)^2} + \frac{6}{r^2}f_\alpha^{(4)^2}\right)\right]\right. \\ + (m_\Delta - m)c^2 f_\alpha^{(1)^2} + 2f_\alpha^{(1)}f_\alpha^{(4)}\langle V_2\rangle \\ \left. + V_\alpha^c f_\alpha^{(1)^2}\right\},\end{aligned} \tag{17}$$

$$a_\alpha^{(1)^2}(r,\rho) = I_J(r,\rho), \tag{18}$$

$$a_\alpha^{(2)^2}(r,\rho) = (2J+1)^{-1}[(J+1)I_{J-1}(r,\rho) + JI_{J+1}(r,\rho)], \tag{19}$$

$$a_\alpha^{(3)^2}(r,\rho) = (2J+1)^{-1}[JI_{J-1}(r,\rho) + (J+1)I_{J+1}(r,\rho)], \tag{20}$$

$$b_\alpha^2(r,\rho) = 2J(J+1)(2J+1)^{-1}[I_{J-1}(r,\rho) - I_{J+1}(r,\rho)], \tag{21}$$

$$I_J(r,\rho) = (2\pi^6\rho^2)^{-1}\int_{|\mathbf{k}_1|,|\mathbf{k}_2|\leqslant k_F} d\mathbf{k}_1 d\mathbf{k}_2 \mathcal{J}_J^2(|\mathbf{k}_1 - \mathbf{k}_2|r). \tag{22}$$

The potential functions $V_\alpha^c, V_\alpha^{\mathcal{T}}, \ldots$, etc., are given in Refs. [3,12].

The normalization constraint as well as the coupled and uncoupled differential equations for the *NN* channels, coming from the Euler-Lagrange equations, are similar to those described in Refs. [3,12]. $\langle V_2\rangle = \langle {}^5D_0|V_2|{}^1S_0\rangle$ is the spin-isospin matrix element of V_2 of the N-Δ transition potential [17] and $\mu(\mu_\Delta)$ is the reduced mass of the N-N (N-Δ) channel. For example, the coupled differential equations for N-Δ channels are

$$\begin{aligned}g_\alpha^{(1)''}(r) - \left\{\frac{a_\alpha^{(1)''}(r)}{a_\alpha^{(1)}(r)} + \frac{2\mu}{\hbar^2}\left[V_1^c - \lambda\right]\right\}g_\alpha^{(1)}(r) \\ - \frac{2\mu}{\hbar^2}\langle V_2\rangle g_\alpha^{(4)}(r) = 0, \\ g_\alpha^{(4)''}(r) - \left\{\frac{a_\alpha^{(1)''}(r)}{a_\alpha^{(1)}(r)} + \frac{2\mu^\Delta}{\hbar^2}[(m_\Delta - m)c^2 - \lambda] + \frac{6}{r^2}\right\}g_\alpha^{(4)}(r) \\ - \frac{2\mu^\Delta}{\hbar^2}\langle V_2\rangle g_\alpha^{(1)}(r) = 0,\end{aligned} \tag{23}$$

with $g_\alpha^{(k)}(r) = a_\alpha^{(k)}f_\alpha^{(k)}(r)$. The boundary conditions for solving these equations are given in Eq. (5) and Refs. [5,10].

Finally, we can also define an effective state averaged two-body potential and correlation function [12] as

$$\mathcal{V}(|\mathbf{r}_1-\mathbf{r}_2|,\rho)=\frac{\sum_{\alpha,i,j,k}\left[(2T+1)(2J+1)\frac{1}{2}\right][1-(-1)^{L+S+T}]\mathcal{V}_\alpha^{j,k}(r,\rho){a_\alpha}^{(i)^2}(r,\rho)}{\sum_{\alpha,i}\left[(2T+1)(2J+1)\frac{1}{2}\right][1-(-1)^{L+S+T}]{a_\alpha}^{(i)^2}(r,\rho)}, \tag{24}$$

$$\mathcal{F}^2(|\mathbf{r}_1-\mathbf{r}_2|,\rho)=\frac{\sum_{\alpha,i}\left[(2T+1)(2J+1)\frac{1}{2}\right][1-(-1)^{L+S+T}]f_\alpha^{(i)^2}(r,\rho){a_\alpha}^{(i)^2}(r,\rho)}{\sum_{\alpha,i}\left[(2T+1)(2J+1)\frac{1}{2}\right][1-(-1)^{L+S+T}]{a_\alpha}^{(i)^2}(r,\rho)}. \tag{25}$$

III. THE MATRIX ELEMENT AND BINDING ENERGY CALCULATIONS

To describe the localized finite nuclei, we no longer have the translation invariance that characterized the nucleon fluid calculations. In this respect, the single-particle wave functions should be determined variationally from

$$\frac{\delta E}{\delta\phi_i}-\epsilon_i\phi_i=0 \tag{26}$$

subject to the constraints $(\phi_i,\phi_j)=\delta_{ij}$, where the single-particle energies ϵ_i are the Lagrange multipliers of the orthogonality constraints. Considering the truncating approximation for the energy in Eq. (10), the above equations become a set of Hartree-Fock equations with the effective two-body interaction $\mathcal{V}_\alpha^{i,j}(r,\rho)$ of Eqs. (15)–(17). But as we stated before, in this work we will not solve Eq. (26), but simply assume that the ϕ_i may be approximated by the harmonic oscillator wave functions, leaving the oscillator energy $\hbar\omega$ as a single variational parameter to fix the rms radius of the nucleus. Here, we assume the following configuration for different closed shell nuclei:

$$\begin{aligned}
&{}^4\mathrm{He}:\left(0s_{\frac{1}{2}}\right)^4\\
&{}^{12}\mathrm{C}:\left(0s_{\frac{1}{2}}\right)^4\left(0p_{\frac{3}{2}}\right)^8\\
&{}^{16}\mathrm{O}:\left(0s_{\frac{1}{2}}\right)^4\left(0p_{\frac{3}{2}}\right)^8\left(0p_{\frac{1}{2}}\right)^4\\
&{}^{28}\mathrm{Si}:\left(0s_{\frac{1}{2}}\right)^4\left(0p_{\frac{3}{2}}\right)^8\left(0p_{\frac{1}{2}}\right)^4\left(0d_{\frac{5}{2}}\right)^{12}\\
&{}^{32}\mathrm{S}:\left(0s_{\frac{1}{2}}\right)^4\left(0p_{\frac{3}{2}}\right)^8\left(0p_{\frac{1}{2}}\right)^4\left(0d_{\frac{5}{2}}\right)^{12}\left(1s_{\frac{1}{2}}\right)^4\\
&{}^{40}\mathrm{Ca}:\left(0s_{\frac{1}{2}}\right)^4\left(0p_{\frac{3}{2}}\right)^8\left(0p_{\frac{1}{2}}\right)^4\left(0d_{\frac{5}{2}}\right)^{12}\left(1s_{\frac{1}{2}}\right)^4\left(0d_{\frac{3}{2}}\right)^8\\
&{}^{56}\mathrm{Ni}:\left(0s_{\frac{1}{2}}\right)^4\left(0p_{3/2}\right)^8\left(0p_{\frac{1}{2}}\right)^4\left(0d_{\frac{5}{2}}\right)^{12}\left(1s_{\frac{1}{2}}\right)^4\left(0d_{\frac{3}{2}}\right)^8\left(0f_{\frac{7}{2}}\right)^{16},
\end{aligned} \tag{27}$$

(Note that ^{12}C, ^{28}Si, and ^{32}S are not magic closed shell. We considered them to see how our method works with these nuclei as well.)

The origin of our coordinate system is fixed at the center of mass of the nucleus, $\sum_{i=1}^{A}\mathbf{r_i}=\mathbf{0}$. Then we should only consider the intrinsic Hamiltonian,

$$H_0=H-\frac{\mathcal{P}^2}{2\mathcal{M}}, \tag{28}$$

where $\mathcal{P}=\sum_i\mathbf{p_i}$ and $\mathcal{M}=Am$ are the nucleus total momentum and mass, respectively.

Now, in the harmonic oscillator basis, we calculate the expectation value of H_0,

$$\begin{aligned}
E_{\mathrm{Total}}^{\mathrm{BE}}=\langle H_0\rangle&=\sum_i\langle i,\hbar\omega|\frac{p^2}{2m}|i,\hbar\omega\rangle\\
&+\frac{1}{2}\sum_{ij}\langle ij,\hbar\omega|\mathcal{V}(12)|ij,\hbar\omega\rangle_a-T_{\mathrm{c.m.}}^A,
\end{aligned} \tag{29}$$

where $T_{\mathrm{c.m.}}^A=\frac{3}{4}\hbar\omega$ and $|i,\hbar\omega\rangle$ stands for $|n_i,l_i,s_i,\tau_i;\hbar\omega\rangle$, the harmonic oscillator wave functions, angular and spin-isospin parts of single-particle states, respectively. $\hbar\omega$ or $\gamma=\sqrt{\frac{m\omega}{\hbar}}$ is the harmonic oscillator parameter and will be fixed variationally, as pointed out before. The matrix element of one-body kinetic energy (first term) has the familiar form

$$T_1^A=\frac{1}{2}\sum_{i=1}^{A}\left(2n_i+l_i+\frac{3}{2}\right)\hbar\omega, \tag{30}$$

while the second term can be written as the sum of two-body kinetic and potential energies

$$\begin{aligned}
E_2^A=T_2^A+V_2^A&=\frac{1}{2}\sum_{ij}\langle ij,\hbar\omega|\mathcal{V}(12)|ij,\hbar\omega\rangle_a\\
&=\frac{1}{2}\sum_{ij}\langle ij,\hbar\omega|-\frac{\hbar^2}{2m}\left\{F(12),\left[\nabla_{12}^2,F(12)\right]\right\}|ij,\hbar\omega\rangle_a\\
&+\frac{1}{2}\sum_{ij}\langle ij,\hbar\omega|F(12)V(12)F(12)|ij,\hbar\omega\rangle_a.
\end{aligned} \tag{31}$$

Then by using (15)–(17), we can write our effective potentials and two-body energy as

$$\mathcal{V}_{\mathrm{eff}}^{k,l}(r_{12},R_{12})=\sum_\alpha\mathcal{V}_\alpha^{k,l}\left[\sqrt{2}r,\rho\left(\frac{R}{\sqrt{2}}\right)\right]|\alpha\rangle\langle\alpha|, \tag{32}$$

with

$$\mathbf{r}=\frac{1}{\sqrt{2}}(\mathbf{r}_1-\mathbf{r}_2)=\frac{1}{\sqrt{2}}\mathbf{r}_{12},\qquad\mathbf{R}=\frac{1}{\sqrt{2}}(\mathbf{r}_1+\mathbf{r}_2)=\sqrt{2}\mathbf{R}_{12}. \tag{33}$$

Next, we have assumed $\alpha=lJST$, $[j]=2j+1$, etc., and first and second curly brackets are the 6-j and 9-j symbols,

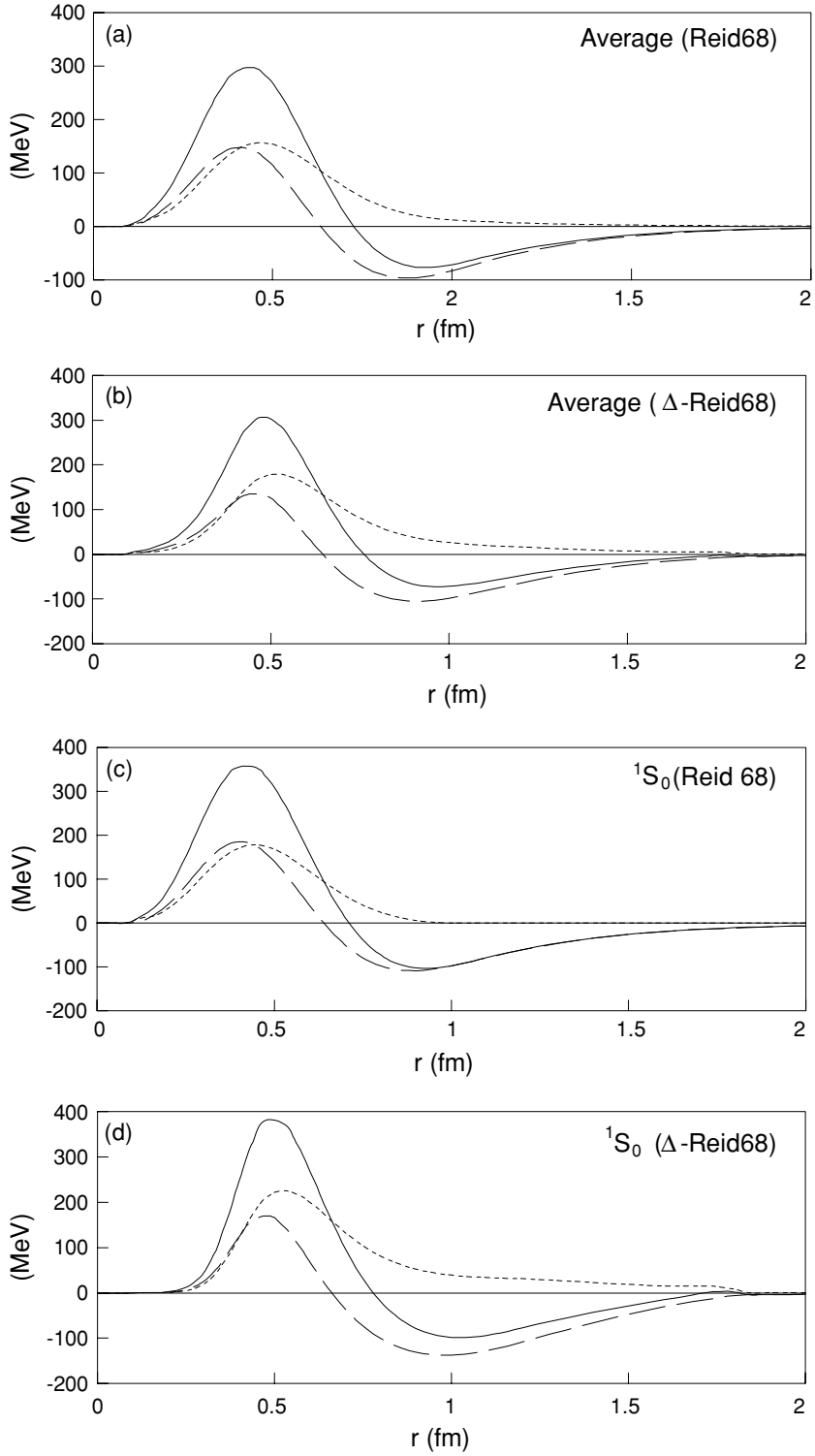

FIG. 1. (a) Averaged two-body effective interaction with Reid68 (full curve) at nuclear matter saturation density, $\rho = 0.17$ fm^{-3}, vs relative distance. (b) Same as (a), but for Δ-Reid68. (c) and (d) are corresponding $^1S_0$-CDEPS, respectively. Dotted and dashed curves are the two-body kinetic and potential parts of the effective interactions.

respectively, in

$$E_2^A = \frac{1}{2}\sum_{1,2,k,l,\alpha'}[j_1][j_2][j][\lambda]^2[S][J][T] \times [1-(-1)^{l+S+T}]\begin{Bmatrix} L & l & \lambda \\ S & j & J \end{Bmatrix}^2 \begin{Bmatrix} l_1 & \frac{1}{2} & j_1 \\ l_2 & \frac{1}{2} & j_2 \\ \lambda & S & j \end{Bmatrix}^2 \times \langle n_1 l_1, n_2 l_2, \lambda | nl, NL, \lambda\rangle^2 \langle nlJST, NL| \mathcal{V}_\alpha^{k,l}\left[\sqrt{2}r, \rho\left(\frac{R}{\sqrt{2}}\right)\right]\{|\alpha'\rangle\langle\alpha'|\}|nlJST, NL\rangle, \quad (34)$$

where we have considered the local density approximation, i.e.,

$$\rho\left(\left|\frac{\mathbf{R}}{\sqrt{2}}\right|\right) = \rho\left(\frac{|\mathbf{r}_1+\mathbf{r}_2|}{2}\right) = \frac{1}{2}[\rho(|\mathbf{r}_1|)+\rho(|\mathbf{r}_2|)]. \quad (35)$$

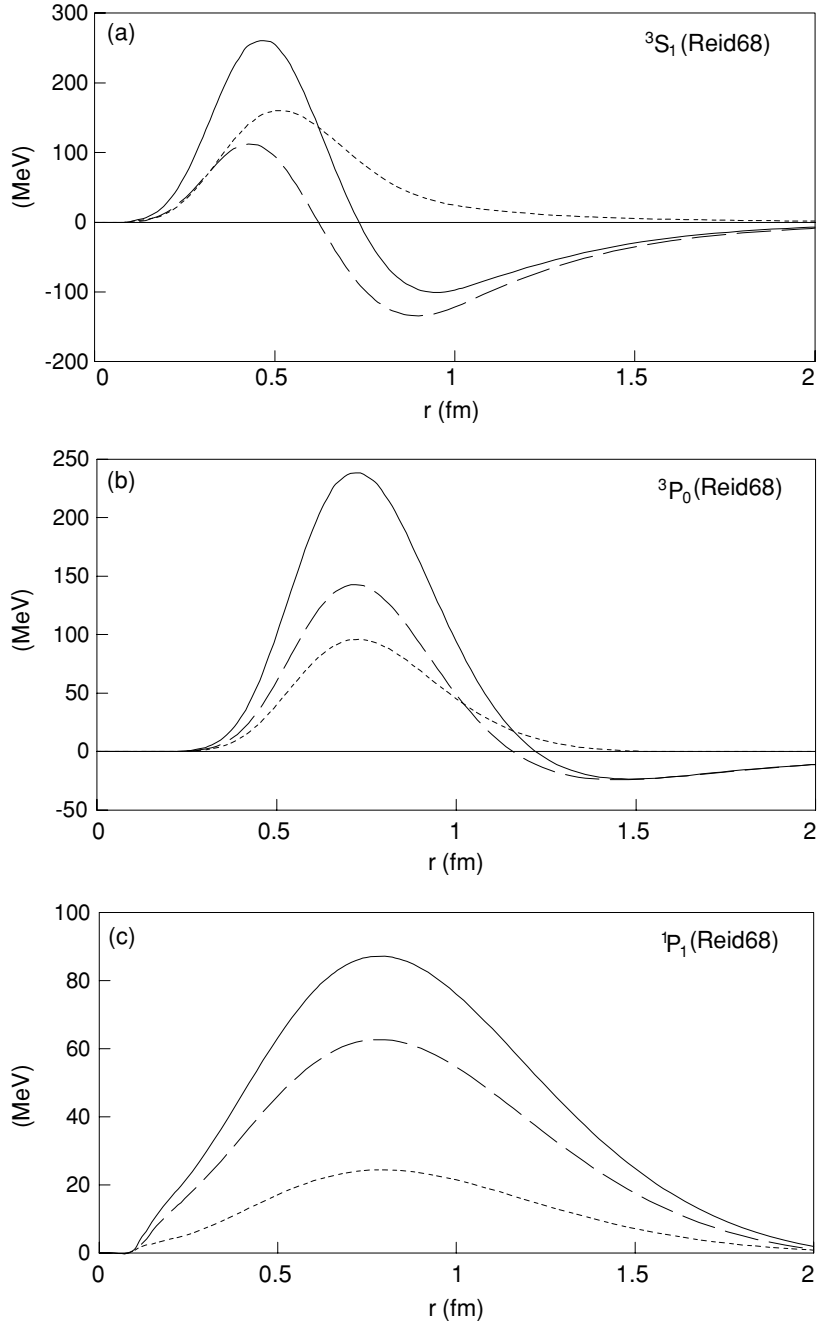

FIG. 2. Same as Fig. 1(c), but for CDEPs of three other channels.

$\langle n_1 l_1, n_2 l_2, \lambda \mid nl, NL, \lambda\rangle$ are the familiar Brody-Moshinsky brackets [24]. The uncorrelated one-body density is defined in terms of the harmonic oscillator wave functions for each nucleus,

$$\rho(\mathbf{r_j}) = \sum_i^A |\langle \mathbf{r_j}|i, \hbar\omega\rangle|^2. \tag{36}$$

We can also define the two-body distribution functions [25] for the above nuclei as

$$\rho_2(\mathbf{r}_1, \mathbf{r}_2) = \rho_2(\mathbf{r}_{12}, \mathbf{R}_{12}) = \frac{1}{A(A-1)}\left[\sum_i^A |\langle \mathbf{r}_1|i, \hbar\omega\rangle|^2 \sum_j^A |\langle \mathbf{r}_2|j, \hbar\omega\rangle|^2 - \left|\sum_i^A \langle \mathbf{r}_1|i, \hbar\omega\rangle \langle i, \hbar\omega, |\mathbf{r}_2\rangle\right|^2\right] \times \mathcal{F}^2[|\ \mathbf{r}_{12}\ |, \rho(|\mathbf{R}_{12}|)], \tag{37}$$

with the correlated one-body density distribution

$$\bar{\rho}(\mathbf{r}_1) = \frac{1}{A-1}\int d\mathbf{r}_2 \rho_2(\mathbf{r}_1, \mathbf{r}_2), \tag{38}$$

and the correlated relative two-body density distribution

$$\bar{\rho}_2(\mathbf{r}_{12}) = \frac{1}{A}\int d\mathbf{R}_{12} \rho_2(\mathbf{r}_1, \mathbf{r}_2). \tag{39}$$

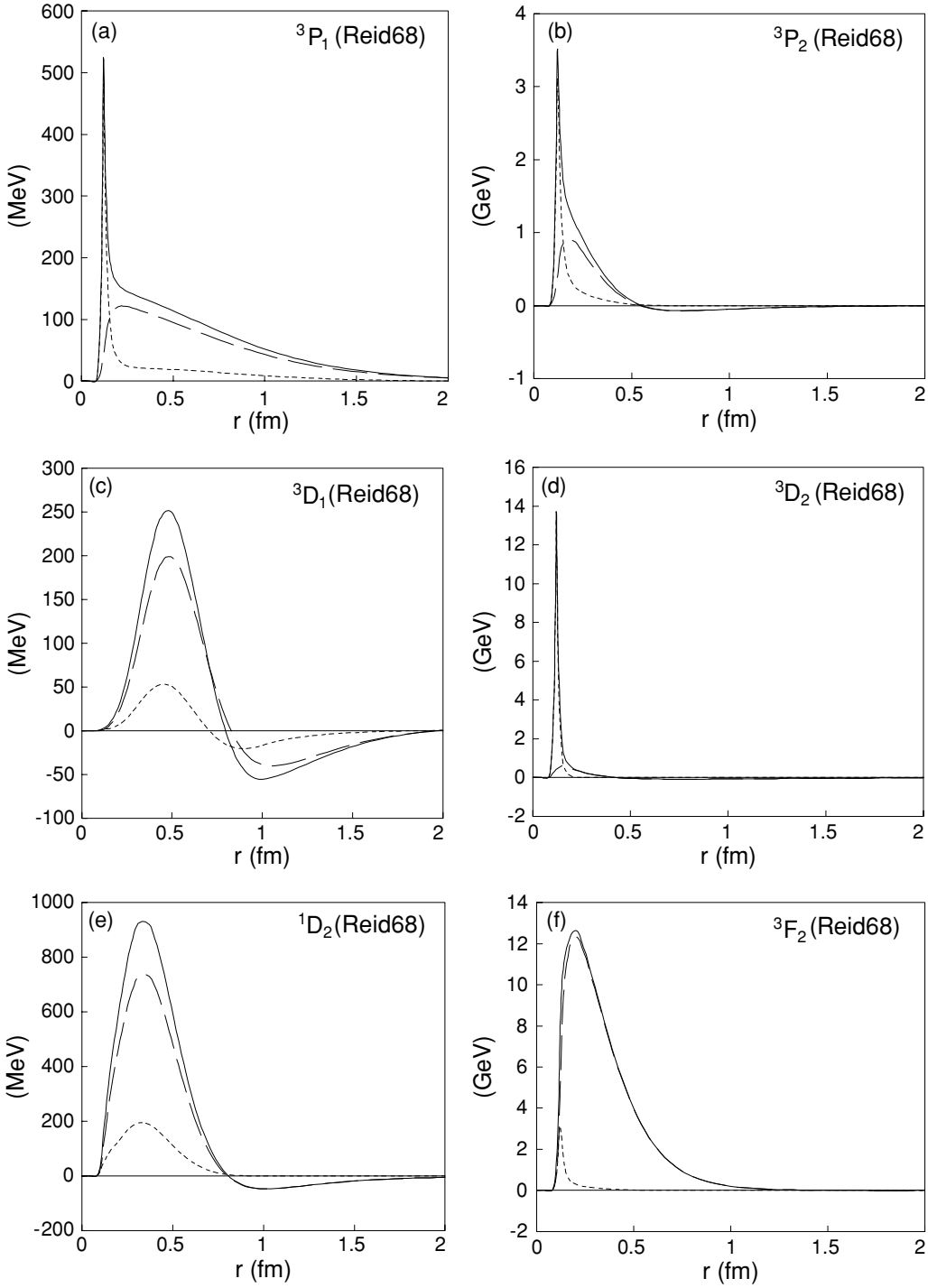

FIG. 3. Same as Fig. 1(c), but for CDEPs of six other channels.

Obviously, we should have the normalization integral,

$$\frac{1}{A(A-1)}\int \rho_2(\mathbf{r}_1,\mathbf{r}_2)d\mathbf{r}_1 d\mathbf{r}_2 = 1. \tag{40}$$

Now, we can easily calculate the nucleus binding energy per nucleon through the equation

$$\mathcal{E}_A^{\rm BE} = \frac{1}{A}E_{\rm Total}^{\rm BE} = \frac{1}{A}\big[T_1^A + T_2^A + V_2^A - T_{\rm c.m.}^A\big]. \tag{41}$$

IV. RESULTS AND DISCUSSION

The results of averaged (AEP) and channel-dependent (CDEP) effective two-body potentials at nuclear matter saturation density $\rho = 0.17$ fm^{-3} for nuclear matter LOCV calculations with Reid68 and Δ-Reid68 potentials are given in Figs. 1–3. The dotted (dashed) curves are the corresponding two-body kinetic (potential) parts of these effective

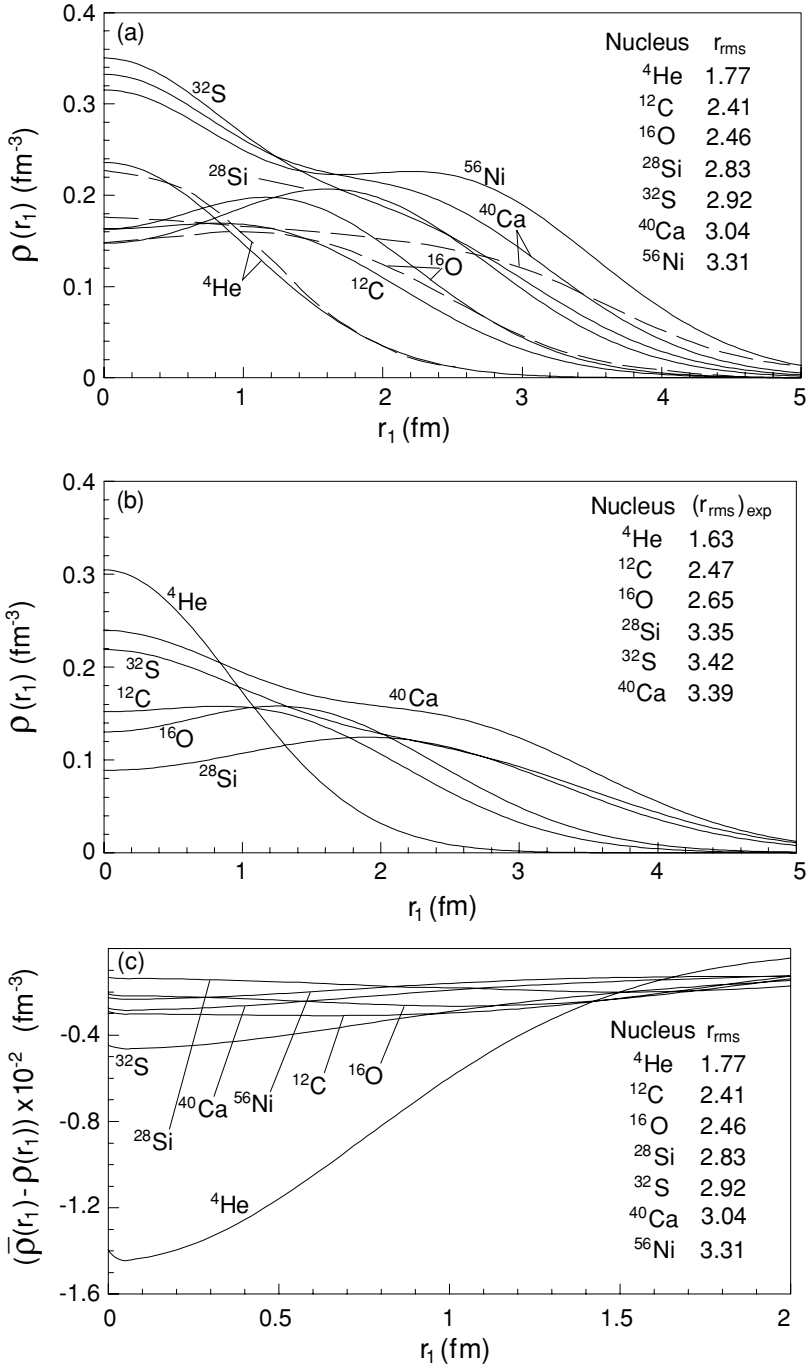

FIG. 4. (a) One-body density for different closed shell nuclei at their saturation points. Dashed curves are the corresponding experimental densities. (b) One-body density at experimental rms radius. (c) Difference between correlated and pure harmonic oscillator one-body densities at our calculated saturation densities.

interactions. From Figs. 1(a) and 1(b), it is seen that the AEP with Δ-Reid68 is more repulsive than the AEP with Reid68, and it has been pushed to the larger values of relative distances. A similar effect can be seen by comparing Figs. 1(c) and 1(d), which plot the effective interactions for the $^1S_0$ channels of Reid68 and Δ-Reid68 interactions. The other CDEPs of Reid68 and Δ-Reid68 are very similar, so we only present those of Reid68 in Figs. 2 and 3. As one expects, the $^1S_0$ and $^3S_1$ CDEPs are very similar, and both have attractive and repulsive parts. Because of the tensor correlation, the kinetic contribution has a longer range in the case of $^3S_1$ CDEP. Its counterpart, $^3D_1$ CDEP, has a similar shape, but its two-body kinetic part becomes attractive for $r \geqslant 0.6$ fm, due to the behavior of the tensor correlation function [3]. The other channels mostly show the repulsive behavior both in their kinetic and potential parts. In general, the $J = 2$ ($\alpha = JLST$) states are strongly repulsive with respect to $J = 0$ and 1 channels.

From Eqs. (35)–(38), the one-body densities are presented in Fig. 4(a) for the closed shell nuclei, i.e., ^{4}He, ^{12}C, ^{16}O, ^{28}Si, ^{32}S, ^{40}Ca, and ^{56}Ni. They have been calculated at their saturation points with the Reid68 potential. The dashed curves

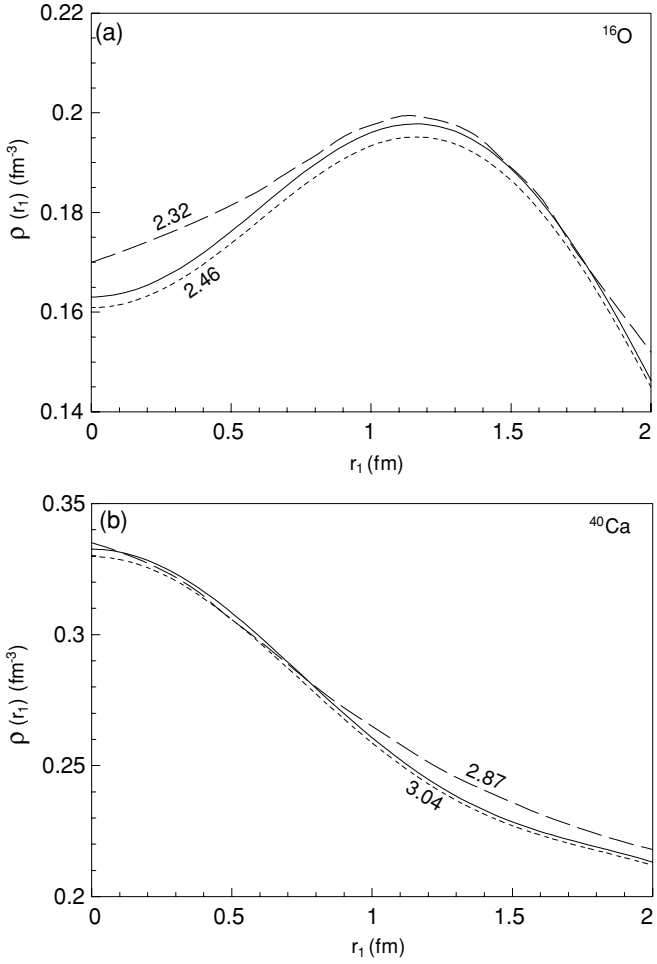

FIG. 5. One-body densities without (full curve) and with (dotted curve) two-body correlation function. Dashed curve is the CBF-FHNC results with the Jastrow correlation function [16].

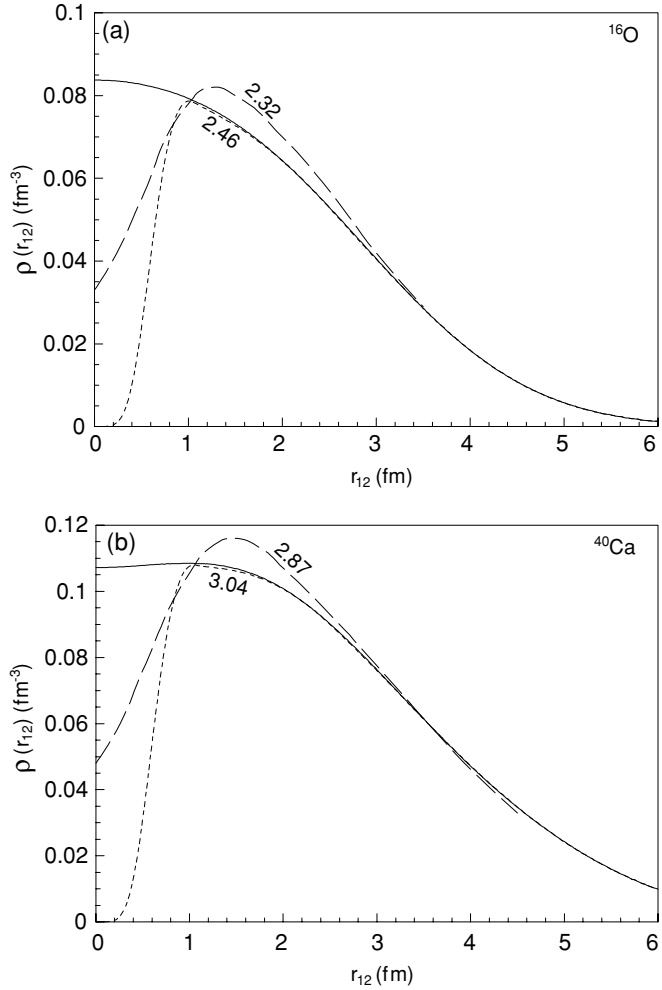

FIG. 6. Same as Fig. 5, but for relative two-body density.

show the available experimental density distributions for ^{4}He, ^{16}O, and ^{40}Ca [19]. For ^{4}He and ^{16}O our calculations give roughly the experimental densities. But for ^{40}Ca because of the small calculated $r_{\rm rms}$ large differences are observed. The corresponding one-body densities obtained by using Eq. (36) at available experimental $r_{\rm rms}$ (charge radius) are given in Fig. 4(b) for comparison with Fig. 4(a) (note that the electromagnetic form factors of nucleons have not been folded into our calculated one-body densities). One can conclude that the pure harmonic oscillator approximation does not give one-body densities close to the experimental prediction. Figure 4(c) shows the difference between the correlated and pure harmonic oscillator one-body densities, i.e., $\bar{\rho}(r_1) - \rho(r_1)$, for different closed shell nuclei at our calculated saturation rms radius. The effect is negligible, especially as we go to heavier nuclei. To make a closer comparison, we compared in Fig. 5 the one-body densities of ^{16}O (at $r_{\rm rms} = 2.46\,$fm) and ^{40}Ca (at $r_{\rm rms} = 3.04\,$fm) obtained by simply using the harmonic oscillator wave function [Eq. (36)] (full curves) with those that were calculated by taking into account the effect of short-range correlations [Eqs. (37) and (38), i.e., $\bar{\rho}(\mathbf{r_1})$] (dotted curves). As pointed out before, we see that there are very small changes in short distances. Obviously, for large distances the effect will be reversed, and it becomes too indistinguishable to be presented in the figure. We tested our normalization integral, i.e., Eq. (40) and found that it is satisfied within 1%. So we can argue that our binding energy calculation will not be affected by the inclusion of a short-range correlation in the one-body density. In other words, the effect of the short-range correlation has already been included in the CDEPs. However, in our future works, we could iterate the one-body density, but we believe this correction will not change our results very much. The results of the CBF-FHNC calculation of Fabrocini *et al.* [16] with the Jastrow correlation and UV_{14} plus three-body interactions have been also given for comparison. In their work, they do not vary the oscillator parameter, but they fix it from the beginning. Their first calculations [16] show that the effect of the correlation function is to reduce the central density. While in their recent work, they claim that the correlation does not change the one-body density significantly. On the other hand, they use the nuclear matter correlation function at some fixed density or they use the nuclear matter density as a variational parameter [16]. The results of Arias de Saavedra *et al.* [16] shows the same phenomena, i.e., no reduction in

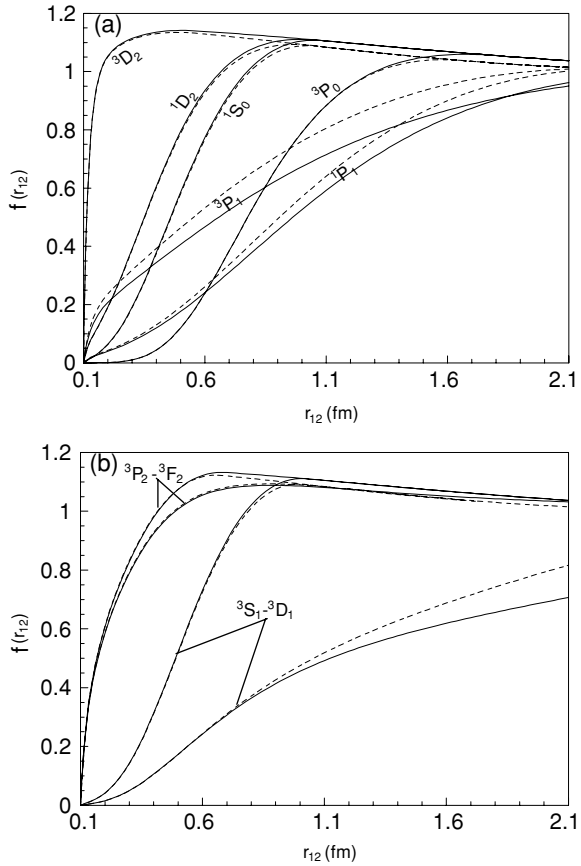

FIG. 7. Channel breakdown of LOCV nuclear matter correlation functions by using Reid68 interaction at two different densities, 0.1 (full curves) and 0.2 fm^{-3} (dotted curves). (a) central and (b) tensor correlation functions.

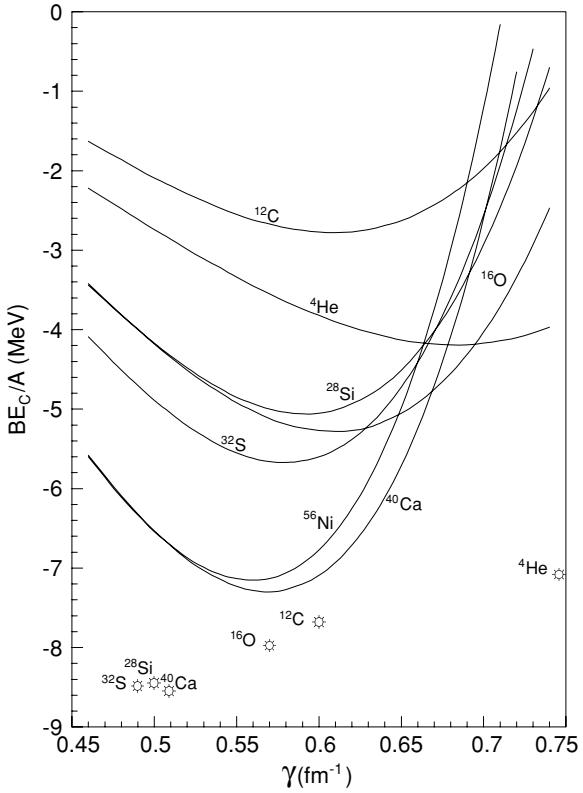

FIG. 8. Saturation curves of closed shell nuclei vs harmonic oscillator parameter γ. Sunburst points are experimental predictions.

the central densities, which contradicts the outcome of CMC calculations [2]. So this behavior should be investigated in detail as has been pointed out in the recent work of Fabrocini *et al*. [16].

Figure 6 shows the two-body relative density distributions in ^{16}O and ^{40}Ca with (dotted curve) and without (full curve) correlation functions. Again the CBF-FHNC calculations of Fabrocini *et al*. [16] are presented for comparison (dashed curve). There is much difference between our calculated correlated relative two-body densities and pure harmonic oscillator ones and those of the CBF-FHNC calculation. Since our correlation functions start from zero, the probability that one nucleon can come close to another one goes to zero. This reflects the effect of nucleon-nucleon interaction at short distances (strong $\frac{1}{r^n}$ behavior). While the CBF-FHNC correlation functions have finite value at $r_{12} = 0$. As we pointed out before, their correlation functions are fixed at some nuclear matter density (they do not depend on the center of mass of two nucleons). We think these center-of-mass-dependent as well as state-dependent ($\alpha = LJST$) considerations are very important. To see this effect in Figs. 7(a) (central) and 7(b) (tensor), we plotted the channel breakdown of our LOCV nuclear matter calculations at two different densities, i.e, 0.1 fm^{-3} (full curves) and 0.2 fm^{-3} (dotted curves), with the Reid68 interaction. Besides the dramatic state-dependent effect, there are also considerable differences between the

TABLE I. Variational binding energies (MeV) of closed shell nuclei obtained by using the AEP in all the channels based on the nuclear matter LOCV calculation with Reid68 interaction. See the text for explanation of different columns.

Nucleus	γ	$\frac{T_1-T_{\text{c.m.}}}{A}$	$\frac{T_2}{A}$	$\frac{V_2}{A}$	$\frac{\text{BE}}{A}$	$\frac{\text{BE}^{\text{exp.}}}{A}$	r_{rms}	$r_{\text{rms}}^{\text{exp.}}$
^{4}He	0.46	4.94	3.34	−8.98	−0.71	−7.08	2.66	1.63
^{12}C	0.50	10.58	6.76	−18.32	−0.98	−7.68	2.94	2.47
^{16}O	0.53	12.56	9.55	−24.87	−2.77	−7.98	2.83	2.65
^{28}Si	0.52	15.32	11.30	−29.87	−3.24	−8.45	3.21	3.35
^{32}S	0.53	16.47	12.86	−33.53	−4.20	−8.49	3.20	3.42
^{40}Ca	0.52	16.61	13.94	−36.32	−5.77	−8.55	3.33	3.39
^{56}Ni	0.52	19.07	15.67	−40.63	−5.89	−8.64	3.56	—

TABLE II. Same as Table I, but for Δ-Reid68.

Nucleus	γ	$\frac{T_1-T_{\text{c.m.}}}{A}$	$\frac{T_2}{A}$	$\frac{V_2}{A}$	$\frac{\text{BE}}{A}$	$\frac{\text{BE}^{\text{exp.}}}{A}$	r_{rms}	$r_{\text{rms}}^{\text{exp.}}$
^{4}He	—	—	—	—	—	−7.08	—	1.63
^{12}C	—	—	—	—	—	−7.68	—	2.47
^{16}O	0.48	10.30	12.25	−23.43	−0.87	−7.98	3.12	2.65
^{28}Si	0.46	11.99	13.70	−26.61	−0.93	−8.45	3.63	3.35
^{32}S	0.48	13.51	16.58	−31.79	−1.70	−8.49	3.53	3.42
^{40}Ca	0.50	15.36	20.84	−39.15	−2.95	−8.55	3.46	3.39
^{56}Ni	0.48	16.25	21.22	−40.34	−2.87	−8.64	3.86	—

TABLE III. Same as Table I, but for CDEP and Reid68.

Nucleus	γ	$\frac{T_1-T_{\rm c.m.}}{A}$	$\frac{T_2}{A}$	$\frac{V_2}{A}$	$\frac{\rm BE}{A}$	$\frac{V_c}{A}$	$\frac{{\rm BE}_c^{J<3}}{A}$	$\frac{{\rm BE}_c}{A}$	$\frac{\rm BE^{exp.}}{A}$	$r_{\rm rms}$	$r_{\rm rms}^{\rm exp.}$
^{4}He	0.69	11.10	9.85	−25.34	−4.38	0.2	−4.19	−4.19	−7.08	1.77	1.63
^{12}C	0.61	15.75	11.37	−30.56	−3.43	0.66	−2.66	−2.78	−7.68	2.41	2.47
^{16}O	0.61	16.64	14.07	−36.89	−6.18	0.9	−5.20	−5.28	−7.98	2.46	2.65
^{28}Si	0.59	19.72	15.71	−41.90	−6.48	1.43	−4.69	−5.06	−8.45	2.83	3.35
^{32}S	0.58	19.72	16.34	−43.32	−7.26	1.59	−5.27	−5.67	−8.49	2.92	3.42
^{40}Ca	0.57	19.96	17.95	−47.11	−9.20	1.91	−6.91	−7.30	−8.55	3.04	3.39
^{56}Ni	0.56	22.12	19.10	−50.77	−9.55	2.40	−6.44	−7.15	−8.64	3.31	—

correlation functions at two different densities, especially the tensor and p-wave correlations. Since in finite nucleus calculations, the nucleus density varies from zero up to 0.3 fm^{-3}, we believe that both the state and center-of-mass dependences are very important.

Tables I and II show the variational binding energies of closed shell nuclei by using the averaged effective interactions in all of the channels with Reid68 and Δ-Reid68 potentials, respectively. For comparison, the calculated and experimental rms radius, one- and two-body kinetic energies, potential energy, oscillator parameter, and experimental binding energy are also given for each nucleus. Clearly, we do not get reasonable results. We get large $r_{\rm rms}$ for lighter nuclei, and there are differences as large as 3–7 MeV difference in the binding energies. The one- and two-body kinetic energies are comparable, and the potential energies are roughly the same as total kinetic energies. The saturation points are worst for the Δ-Reid68 potential, and we do not find any bound states for ^{12}C and ^{4}He.

Tables III and IV are similar to Tables I and II, but they reflect the nuclear matter CDEPs. For channels with $J \geqslant 3$, we used the averaged effective interaction. Here, there are also three additional columns giving the Coulomb potential, binding energies with zero effective interactions in channels with $J \geqslant 3$, and binding energies with Coulomb interaction. We get reasonable $r_{\rm rms}$ with respect to the experimental data for the whole range of closed shell nuclei. The binding energies are close to their corresponding experimental values as the nuclear mass increases, especially with the Reid68 interaction. The one- and two-body kinetic energies have roughly the same size, and two-body potential energies are also roughly twice each of them. The contributions of $J \geqslant 3$ channels are negligible. Again the results of binding energy calculation with Reid68 is much closer to the experimental data than the Δ-Reid potential. Our total and two-body kinetic as well as potential and Coulomb energies are very close to those of CBF-FHNC for ^{16}O and ^{40}Ca [16] and CMC for ^{16}O [2].

To see how much our results vary with respect to the harmonic oscillator parameter, i.e., rms radius, the saturation curves of binding energies per nucleon for the closed shell nuclei are given in Fig. 8. For larger nuclei, the saturation point goes to lower energy and smaller harmonic oscillator parameter γ or larger $r_{\rm rms}$, except for ^{12}C, which has a small size and is not a perfect closed shell nucleus. The saturation curves are sensitive to γ. This indicates that one should take a wider range of harmonic oscillator wave functions as the single-particle states [including all of the principle quantum number pairs (n_1, n_2)].

Finally, in Table V, we compare our calculated binding energy and rms radius for ^{4}He, ^{16}O, and ^{40}Ca with different approaches, namely, the coupled cluster of Kümmel *et al.* [15], cluster (variational) Monte Carlo of Pieper *et al.* [2], CBF-FHNC of Fabrocini *et al.* [16], Brueckner-Hartee-Fock of Coraggio *et al.* [17] with N^3LO and AV_{18} interactions, and Fermionic molecular dynamics of Roth *et al.* [18]. The CCM calculation is with Reid68, while the other methods used UV_{14} or AV_{18} plus the three-body interaction (TBI). We have not included TBI in our calculation. Its contribution is about a MeV binding. So by comparison we can conclude that we get reasonable results especially for ^{40}Ca with respect to both experimental data and other theoretical calculations. It is worth saying that for each harmonic oscillator parameter, the calculation for ^{40}Ca takes about 20 min. on a Pentium IV 2400 MHz

TABLE IV. Same as Table I, but for CDEP and Δ-Reid68.

Nucleus	γ	$\frac{T_1-T_{\rm c.m.}}{A}$	$\frac{T_2}{A}$	$\frac{V_2}{A}$	$\frac{\rm BE}{A}$	$\frac{V_c}{A}$	$\frac{{\rm BE}_c^{J<3}}{A}$	$\frac{{\rm BE}_c}{A}$	$\frac{\rm BE^{exp.}}{A}$	$r_{\rm rms}$	$r_{\rm rms}^{\rm exp.}$
^{4}He	0.64	9.55	13.99	−25.87	−2.32	0.18	−2.14	−2.14	−7.08	1.91	1.63
^{12}C	0.55	12.80	14.81	−28.64	−1.02	0.58	−0.37	−0.44	−7.68	2.68	2.47
^{16}O	0.57	14.52	20.07	−37.81	−3.21	0.83	−2.33	−2.38	−7.98	2.63	2.65
^{28}Si	0.55	17.13	22.21	−42.52	−3.18	1.30	−1.63	−1.89	−8.45	3.03	3.35
^{32}S	0.54	17.10	23.04	−43.97	−3.83	1.43	−2.13	−2.40	−8.49	3.14	3.42
^{40}Ca	0.54	17.91	26.49	−49.85	−5.45	1.91	−3.41	−3.69	−8.55	3.21	3.39
^{56}Ni	0.53	19.81	28.11	−53.48	−5.56	2.19	−2.86	−3.37	−8.64	3.49	—

TABLE V. Comparison of ground state binding energies per nucleon (MeV) and rms radius (fm) of ^{4}He, ^{16}O and ^{40}Ca nuclei with different models and experimental data.

	^{4}He		^{16}O		^{40}Ca	
	$\frac{BE}{A}$	$\langle r \rangle$	$\frac{BE}{A}$	$\langle r \rangle$	$\frac{BE}{A}$	$\langle r \rangle$
CCM (FBHF3), Kummel [15]	−5.75	1.63	−5.36	2.57	−5.64	3.17
CMC, Pieper [2]	−7.6	—	−7.7	—	—	—
CBF-FHNC, Fabrocini (1998) [16]	—	—	−5.15	2.32	−7.87	2.87
CBF-FHNC, Fabrocini (2000) [16]	—	—	−5.11	2.93	−6.50	3.66
BHF, Coraggio (2003) [17]	—	—	−7.52	2.65	−9.19	3.44
BHF, Coraggio (2005) [17]	−6.85	1.69	−8.26	2.59	−9.53	3.22
FMD, Roth [18]	−6.99	1.51	−7.40	−2.25	−8.19	2.89
LOCV (Reid68)	−4.19	1.77	−5.28	2.46	−7.30	3.04
Experimental	−7.08	1.63	−7.98	2.65	−8.55	3.39

personal computer. This can be, for example compared with a CMC calculation estimated to take at least 10 h. of time on a Cray-2 super computer.

In conclusion, we have calculated the binding energy of light closed shell nuclei by considering the local density approximation and the effective interaction which were calculated by using a reliable method such as LOCV formalism with Reid68 and Δ-Reid68 potentials. One can argue that we do not know the accuracy of the above approximations, especially the truncation we imposed on the configuration space. However, it is encouraging that our results are in agreement with those of methods that use more complicated formalism and computer simulation. Our binding energy results with the Reid68 interaction become closer to the experimental data as we go to the heavier light nuclei. So we can conclude that we may get more reasonable results if we apply our method to heavier nuclei.

We can improve our result by (i) taking into the account the TBI, (ii) using the new charge-dependent potential and our asymmetrical nuclear matter code, and (iii) including the averaged three-body cluster effective interaction into the present two-body channel-dependent effective potential.

Finally, we would like to make the general remark that in any cluster expansion calculation, the choice of many-body correlation function and satisfaction of the normalization integral is much more important than considering the higher order many-body cluster energies such as the one usually performed in different FHNC calculations [26], especially for nuclear matter.

ACKNOWLEDGMENTS

M.M. would like to thank University of Tehran for supporting him under the grants provided by its Research Council. N.R. thanks Dr. Moshfegh for many useful discussions.

[1] C. R. Chen, G. L. Payne, J. L. Friar, and B. F. Gibson, Phys. Rev. C **33**, 1740 (1986); A. Stadler, W. Glöckle, and P. U. Sauer, *ibid.* **44**, 2319 (1991).

[2] J. Carlson, Phys. Rev. C **38**, 1879 (1988); S. C. Pieper, R. B. Wiringa, and V. R. Pandharipande, *ibid.* **46**, 1741 (1992); B. S. Pudliner, V. R. Pandharipande, J. Carlson, S. C. Pieper, and R. B. Wiringa, *ibid.* **56**, 1720 (1997); A. Kievsky, M. Viviani, and S. Rosati, Nucl. Phys. **A551**, 241 (1993); S. C. Pieper, R. B. Wiringa, and J. Carlson, Phys. Rev. C **70**, 054325 (2004); S. C. Pieper, Phys. Rev. Lett. **90**, 252501 (2003); S. C. Pieper, K. Varga, and R. B. Wiringa, *ibid.* **66**, 044310 (2002); S. C. Pieper and R. B. Wiringa, Annu. Rev. Nucl. Part. Sci. **51**, 53 (2001).

[3] J. C. Owen, R. F. Bishop, and J. M. Irvine, Ann. Phys. (NY) **102**, 170 (1976); M. Modarres and J. M. Irvine, J. Phys. G **5**, 511 (1979); M. Modarres and G. H. Bordbar, Phys. Rev. C **58**, 2781 (1998); R. V. Reid, Ann. Phys. (NY) **50**, 411 (1969).

[4] B. D. Day, Rev. Mod. Phys. **50**, 495 (1978); J. W. Clark, Prog. Part. Nucl. Phys. **2**, 89 (1979); V. R. Pandharipande and R. B. Wiringa, Rev. Mod. Phys. **51**, 821 (1979).

[5] B. Friedman and V. R. Pandharipande, Nucl. Phys. **A361**, 502 (1981); R. B. Wiringa, V. Ficks, and A. Fabrocini, Phys. Rev. C **38**, 1010 (1988); V. R. Pandharipande and R. B. Wiringa, Rev. Mod. Phys. **51**, 821 (1979).

[6] M. Modarres and J. M. Irvine, J. Phys. G **5**, 7 (1979).

[7] I. E. Lagaris and V. R. Pandharipande, Nucl. Phys. **A359**, 331 (1981).

[8] R. B. Wiringa, R. A. Smith, and T. L. Ainsworth, Phys. Rev. C **29**, 1207 (1984).

[9] R. B. Wiringa, V. G. J. Stoks, and R. Schiavilla, Phys. Rev. C **51**, 38 (1995).

[10] V. Stoks and J. J. de Swart, Phys. Rev. C **52**, 1698 (1995).

[11] K. E. Schmidt and V. R. Panharipande, Phys. Lett. **B87**, 11 (1979); A. Akmal, V. R. Pandharipande, and D. G. Ravenhall, Phys. Rev. C **58**, 1804 (1998).

[12] M. Modarres and J. M. Irvine, J. Phys. G **5**, 7 (1979); M. Modarres, J. Phys. G **19**, 1349 (1993); M. Modarres and H. R Moshfegh, Phys. Rev. C **62**, 044308 (2000); G. H. Bordbar and M. Modarres, J. Phys. G: Nucl. Part. Phys. **23**, 1631 (1997); Phys. Rev. C **57**, 714 (1998); H. R. Moshfegh and M. Modarres, J. Phys. G **24**, 821 (1998).

[13] R. F. Bishop, C. Howes, J. M. Irvine, and M. Modarres, J. Phys. G **4**, 1709 (1978).
[14] M. Modarres, J. Phys. G **10**, 251 (1984).
[15] H. Kümmel, K. H. Lührmann, and J. G. Zabolitzky, Phys. Rep. **36**, 1 (1978).
[16] A. Fabrocini, F. Arias de Saavedra, G. Có, and P. Folgarait, Phys. Rev. C **57**, 1668 (1998); A. Fabrocini, F. Arias de Saavedra, and G. Có, *ibid*. **61**, 044302 (2000); F. Arias de Saavedra, G. Có, and M. M. Renis, *ibid.* **55**, 673 (1997); G. Có, A. Fabrocini, S. Fantoni, and E. Lagaris, Nucl. Phys. **A549**, 439 (1992); G. Có, A. Fabrocini, and S. Fantoni, *ibid*. **A568**, 73 (1992).
[17] L. Coraggio, N. Itaco, A. Covello, A. Gargano, and T. T. S. Kuo, Phys. Rev. C **68**, 034320 (2003); L. Coraggio, A. Covello, A. Gargano, N. Itaco, T. T. S. Kuo, and R. Machleidt, *ibid*. **71**, 014307 (2005).
[18] R. Roth, T. Neff, H. Hergert, and H. Feldmeier, Nucl. Phys. **A745**, 3 (2004).
[19] H. de Vries, C. W. de Jager, C. de Vries, At. Data Nucl. Data Tables **36**, 496 (1987).
[20] V. Stoks and J. J. de Swart, Phys. Rev. C **47**, 761 (1993); **52**, 1698 (1995); V. G. J. Stoks, R. A. M. Klomp, C. F. P. Terheggen, and J. J. de Swart, *ibid*. **49**, 2950 (1994); V. G. J. Stoks, R. A. M. Klomp, M. C. M. Rentmeester, and J. J. de Swart, *ibid*. **48**, 792 (1993).
[21] A. M. Green, J. A. Niskanan, and M. E. Sainio, J. Phys. G **4**, 1085 (1978).
[22] M. Modarres, J. M. Irvine, and R. F. Bishop, J. Phys. G **4**, 127 (1978).
[23] M. Modarres and H. R. Moshfegh, Prog. Theor. Phys. **112**, 21 (2004); H. R. Moshfegh and M. Modarres, Nucl. Phys. **A** (to be published).
[24] T. Brody and M. Moshinsky, *Tables of Transformation Brackets* (Mexico Instituto de Fisica, 1960).
[25] E. Feenberg, *Theory of Quantum Fluids* (Academic Press, New York, 1969); M. A. Preston and R. K. Bhaduri, *Structure of the Nucleus* (Addison-Wesley, Reading, MA, 1975).
[26] M. Modarres, H. R. Moshfegh, K. Fallahi, Eur. Phys. J. B **36**, 465 (2003); M. Modarres, J. Low Temp. Phys. **139**, 358 (2005).